Hindawi
Shock and Vibration
Volume 2019, Article ID 4067915, 11 pages
https://doi.org/10.1155/2019/4067915

Research Article

Seismic Design of Bridges against Near-Fault Ground Motions Using Combined Seismic Isolation and Restraining Systems of LRBs and CDRs

Xiaoli Li[1] **and Yan Shi**[2]

[1]*Institute of Road and Bridge Engineering, Dalian Maritime University, Dalian 116026, China*
[2]*School of Civil Engineering, Lanzhou University of Technology, Lanzhou 730050, China*

Correspondence should be addressed to Xiaoli Li; lxl_0916@dlmu.edu.cn

Received 14 December 2018; Revised 13 February 2019; Accepted 18 March 2019; Published 7 April 2019

Academic Editor: Jean-Jacques Sinou

This paper focuses on the seismic isolation design of near-fault bridges under the seismic excitations of near-fault ground motions in high-intensity earthquake zones and proposes a combined control system using lead rubber bearings (LRBs) and cable displacement restrainers (CDRs) along with ductility seismic resistance for the reinforced concrete piers. As part of the performance-based seismic design framework, this study provides the quantitative design criteria for multilevel performance-based objectives of a combined control system under conditions of frequent earthquake (E1), design earthquake (medium earthquake), and rare earthquake (E2). Moreover, in this study, a preliminary performance-based seismic isolation design for a near-fault actual highway bridge in high-intensity earthquake zones (basic peak of ground acceleration 0.4 g) was developed. Using nonlinear time-history analysis of the actual bridge under near-fault ground motions, the feasibility of a performance-based design method was validated. Furthermore, to ensure the predicted performance of the isolated bridges during a strong earthquake, a relatively quantitative design in structural details derived from the stirrup ratio of piers, expansion joints gap, supported length of capping beams, and limited vertical displacement response was obtained.

1. Introduction

Since the 1970s, seismic isolation technology has been applied to bridge engineering, and it has been used increasingly in bridge design and strengthening in meizoseismal areas. Although the seismic isolation technology of bridges was developed late in China, the number of isolated bridges has grown from few dozens to near one thousand after the Wenchuan Earthquake in 2008 (oral research reports of Prof. F. L. Zhou). Presently, the development of transportation infrastructure in China, such as high-speed rail and highway transportation facilities, has been making great progress and improved rapidly. In fact, some highway bridges in high-intensity earthquake zones with a peak of ground acceleration (PGA) of >0.4 g and near active fault sites were constructed in Yunnan, Tibet, Gansu, and other western provinces of China. Near-fault ground motions are different from ordinary ground motions in that they often contain strong coherent dynamic long-period pulses and permanent ground displacements ("fling step"). The dynamic motions are dominated by a large long-period pulse of motion that occurs usually on the horizontal component perpendicular to the strike of the fault, caused by rupture directivity effects. The static ground displacements in near-fault ground motions are caused by the relative movement of the two sides of the fault on which the earthquake occurs. These displacements are discontinuous across a fault having surface rupture and can subject a bridge crossing a fault to significant differential displacements [1]. At present, seismic isolation technology [2, 3] is being extensively used in near-fault bridges such as the Turkey

Bolu Viaduct, Iceland Thjorsa River Bridge, and Oseyrar Bridge, all of which have withstood the test of near-fault ground motions during real earthquakes [4–7]. Although those bridges had suffered some damage, they also showed that seismic isolation still has some positive effects under the near-fault ground motions with velocity pulse effects. If the seismic isolation design was not adopted, the damage would have been more extensive. Studies related to seismic disasters indicate that near-fault ground motions will cause large displacements of bridges at the earlier stage and that the energy-dissipating function of the seismic isolation elements is not completely developed and they will be damaged early during the earthquake. Unless the size and the capacity of seismic isolation elements are larger, they will decrease the economic efficiency of the isolation design of bridges. Therefore, combining the elastic or plastic displacement-restoring devices with seismic isolation devices can be considered as an important measure. For example, Diclei [8, 9] utilized additional elastic stiffness or elastic-gap devices, and Osman et al. [10] utilized SMA (shape memory alloy, SMA) connection devices. Usually very large displacements make seismic isolation an unfeasible solution due to boundary conditions, especially in case of existing bridges or high-risk seismic regions. Losanno et al. [11, 12] implemented a frequency domain approach for damping optimization in both elastomeric viscoelastic and sliding isolators on regular bridges and demonstrated that increasing the damping level of the isolation system is not always favorable, and there exists an upper limit for the damping level, after which they presented a numerical investigation on the seismic behavior of isolated bridges with supplemental viscous damping under near-fault strong motions.

"Guidelines for Seismic Design of Highway Bridge" in China (JTG/T B02-01-2008) [13] only provides simple avoidance principles and general guidance for near-fault bridge design and lacks detailed quantitative calculations and detailed design requirements. Therefore, there are few issues in seismic design of bridges subjected to near-fault ground motions. In addition to practical engineering projects, a combined control system with lead rubber bearings (LRBs), cable displacement restrainers (CDRs), and ductility seismic design of bridge piers was proposed. Furthermore, a numerical model based on OpenSees for seismic analysis was established. According to multilevel performance objectives, performance-based seismic isolation design of near-fault highway bridges in high-intensity earthquake zones was achieved.

2. Bridge Project Background

A 260 m ($4 \times 20 + 5 \times 20 + 4 \times 20$ m) continuous girder bridge in Yunnan province was studied. The bridge's superstructures consist of five prefabricated small box girders placed abreast. The width of the single girder is 3.1 m and the substructures comprised reinforced concrete double-column piers, whose height ranges from 5 to 9 m. The rectangular section of columns is designed as 1.4 m long by 1.4 m wide. The prefabricated small box girders and end transverse girders utilized C50 concrete, whereas the cap beams, blocks, link girders, and piers are constructed of C40 concrete. Figure 1 shows the elevation and transverse section of the bridge.

Note that the seismic intensity of the bridge is IX degree, and the basic design ground motion acceleration is 0.4 g. Furthermore, the bridge is located in the site near the western branch of Xiaojiang Fault, and the distance between them is less 10 km. The site category is III with a potential seismic risk of magnitude 7.0. Note that the maximum earthquake recorded was a magnitude 8.0 earthquake at Songming Yangling in 1833.

3. Seismic Isolation Scheme and Performance-Based Design Objectives

3.1. Bridge Seismic Isolation Scheme. For medium earthquakes, the basic PGA for this bridge is 0.4 g; however, for larger earthquakes, the PGA could be >0.6 g. Moreover, it is necessary to consider the long-period impulse effect of near-fault ground motions. As shown in Figure 2, this paper proposed a highway bridge isolation design scheme with a combined control system of LRBs and CDRs, in addition to a ductility seismic design of bridge piers. First, the yield and energy dissipation of LRBs were used to protect the bridge piers (I). When the bearing was close to its limit of deformation capacity, the CDRs (mature commercially available products that are widely used in the world) worked (II). When the bridge was subjected to the extreme ground motions (e.g., near-fault ground motions), the bridge piers could have a plastic response with ductility and the collapse should be avoided (III). The stirrups and other construction measures can ensure its ductile seismic-resistant capacity. Using such schemes, a step-by-step fortification can be achieved, and the seismic isolation design, ductility design, and displacement control can be systematically unified to prevent bridge collapse under a strong earthquake close to the active fault.

3.2. Multilevel Performance-Based Seismic Design Objectives. Focusing on the abovementioned scheme, we proposed the seismic isolation and multilevel performance-based design of near-fault bridges in high-intensity earthquake zones, which was defined as follows.

E1 earthquakes (small earthquakes): piers remain elastic, seismic isolation bearings were allowed to yield, the maximum shear strain of rubber-type bearings should be less than 100%, and the residual displacement which would cause a negative effect on usage should not be generated. Note that the residual displacement should be controlled within 10%–15% of the bearing height. This value was based on the assumption that the thickness of rubber layer was 0.6 times as high as the bearing height. Furthermore, a design value, 250%, was adopted as the maximum shear strain. According to the introduction [14, 15] of Japanese seismic isolation bridge design requirements by Kawashima, when the deformation displacement reaches the design

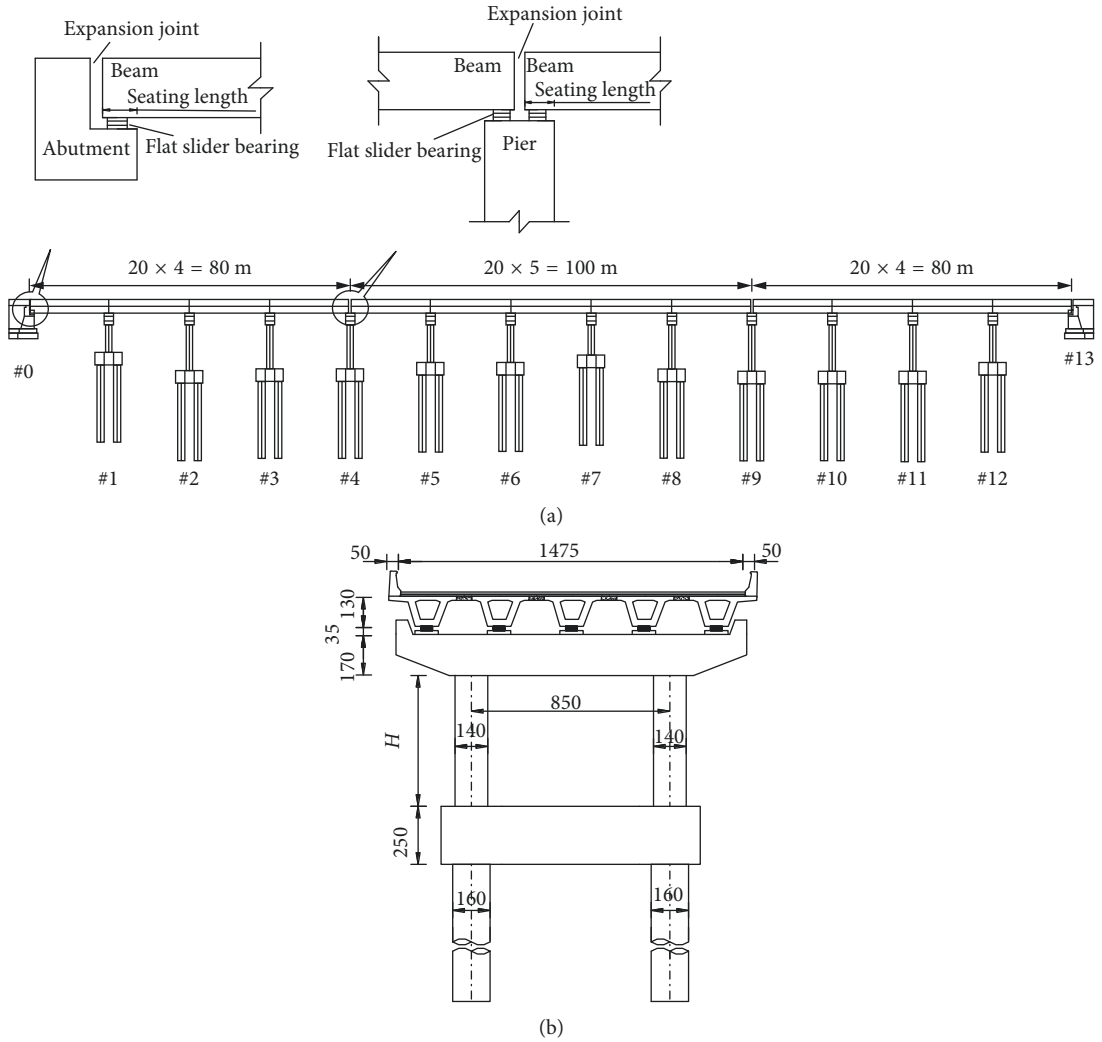

Figure 1: Elevation and transverse section of the bridges. (a) Elevation (unit: cm). (b) Transverse section (unit: cm).

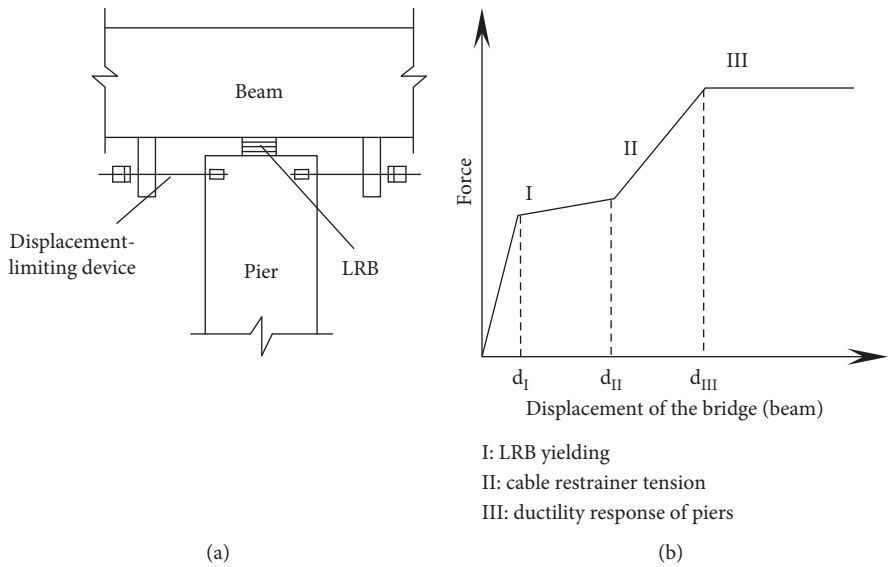

Figure 2: Scheme of the combined isolation system. (a) Combined isolation system. (b) Restoring force and displacement response schematic.

displacement u_B, in the condition of slow release, the residual displacement should satisfy the inequality $u_{BR} \le 10\% u_B$. Thus, the maximum residual displacement calculated by a simple bilinear hysteretic model should be less than 15% of the bearing height.

Design earthquakes (medium earthquakes): piers were allowed to yield; the yield strength of piers was greater than the yield strength of the bearings (i.e. $F_{Py} > F_{By}$), which could ensure the bearings yield first. The residual crack width of piers should be sufficiently small, and no repair is required after the earthquake. It can be controlled by damage index, such as the displacement ductility coefficient which can be confined with 1.2 to 1.5, and by the compressive strain of the constrained concrete (within $\varepsilon_{cu} = 0.0033$).

E2 earthquakes (large earthquakes): piers were allowed to yield but the damage should be controlled, and the bridge should not collapse. By controlling the amount of stirrups, the limited drift ratio of piers could not exceed 3%. Furthermore, the maximum shear strain of the LRBs should be 250%.

Some brief descriptions about E1 and E2 earthquake risk levels had been presented. As stipulated by various specifications in China, Table 1 listed the E1 and E2 earthquake effects in regions with a basic PGA value of 0.4 g. In this study, the peak accelerations of 0.2 g for E1 earthquakes, 0.4 g for medium earthquakes, and 0.62 g for E2 earthquakes were adopted.

4. Bridge Seismic Isolation Design and Performance Assessment

Based on the displacement-based seismic design method of medium-span seismic isolation bridge developed by Shi et al. [16], seismic isolation was performed for every continuous unit under medium earthquakes. Then, to adjust the multilevel performance of the overall structure (three continuous units), the time-history analysis was conducted. In this study, the seismic isolation design in the bridge's longitudinal direction had been investigated; moreover, the bidirectional seismic isolation had been described [16].

The seismic isolation-bearing layout of this bridge was designed as follows: LRBs were installed on the piers of continuous spans, and flat slider bearings with larger displacement capacities were arranged at the bridge abutment and expansion joints. The reason for adopting this layout was that the bearings at the bridge abutment and expansion joints had larger displacement requirements during earthquakes. The bearings at abutments and expansion joints usually had larger displacement requirements because of the difference of dynamic characteristics and discontinuous displacement between adjacent structures in the continuous girder spanning over multisupports, which was also confirmed by the earthquake damages of several isolated bridges during the Great East Japan Earthquake on March 2011. The seismic design of the combined seismic isolation systems with LRBs and CDRs was carried out based on seismic design code, technical standard of isolated bearings, and displacement-based seismic design method [16]. The formulas of equivalent damping ratio and the effective period [16] of bridge system were as follows:

$$\xi_{eff} = \frac{\sum_1^n \left(m_i \cdot \xi_{eff,i}\right)}{\sum_1^n m_i},$$
$$T_{eff} = 2\pi \sqrt{\frac{M_{eff}}{K_{eff}}}. \quad (1)$$

The bridge was designed based on the "Guidelines for Seismic Design of Highway Bridge" in China (JTG/T B02-01-2008), and the design spectra (see Figure 3 as reference) with the basic PGA equaling to 0.4 g was adopted. The equivalent damping ratios were 32%, 30%, and 32%, and the effective periods were 1.71 s, 1.75 s, and 1.73 s by calculating for the three segments from left to the right of the bridge (see Figure 1)when the same target displacements of 0.16 m for the bridge beams were considered. Moreover, according to the requirements of vertical bearing capacity and horizontal bearing capacity of the bearings, the appropriate bearings were selected in the products of isolation bearings [17]. Finally, the model number of lead rubber bearing was Y4Q770 × 232 with the total rubber layer height 144 mm. The model number of flat slider bearing at the abutment and pier expansion joints was $GYZF_4D400 \times 60$ and $GYZF_4D400 \times 38$, respectively. The corresponding mechanical parameters are shown in Table 2. K_1, K_2, and F_y represented the preyielding stiffness, postyielding stiffness, and (level) yield strength of the bearing system at the bridge pier, respectively. Furthermore, [F] represented the vertical capacity of the bearings in the seismic isolation technique specifications [17].

Cable displacement restrainers were installed at both sides of the box girders and were anchored to the bridge's piers (capping beam). Note that their initial gap was 0.28 m (i.e., it worked when the bearing shear strain $\gamma = 200\%$). There were 5 restrainers in total on one side of the bridge's superstructure which were composed of five prefabricated small box girders. A schematic drawing of the commercial CDR system was presented in Figure 4, whose yield force was 1540 kN with an axial stiffness of 1.7×10^4 kN/m (the total axial stiffness of the cables at one side of the bridge substructures was 8.5×10^4 kN/m). The arrangement of all devices is also shown in Figures 1 and 2.

Based on these calculations, reinforcement of the section for bridge piers was appropriately adjusted and arranged, as shown in Figure 5. HRB400 longitudinal reinforcement consisted of Φ28, HRB400 stirrup consists of Φ14 limb stirrup, and both of them were longitudinally and transversely installed. The yield strength of HRB400 steel is 400 MPa. L_p represented the length of the mesh area of the confined steel bars in equivalent plastic hinge, and L_p was determined according to the "Guidelines for Seismic Design of Highway Bridge" in China (JTG/T B02-01-2008). In Figure 5, the parameter n represented the number of stirrups.

Table 1: Earthquake risk levels for PGA.

Specification	E1 (small earthquake)	Design earthquake (medium earthquake)	E2 (rare earthquake)
Guidelines for seismic design of highway bridge (JTG/TB02-01-2008)	0.2 g	0.4 g	0.68 g
Code for seismic design of urban bridge (CJJ166-2011)	0.24 g	0.4 g	0.62 g
Code for seismic design of buildings (GB50011-2010)	0.14 g	0.4 g	0.62 g
Code for seismic design of urban rail transit structures (GB50909-2014)	0.14 g	0.4 g	0.62 g
Code for seismic design of railway engineering (GB50111-2006, 2009 local revised edition)	0.16 g	0.4 g	0.64 g

Note. Importance coefficient has been corrected according to the situation of this bridge.

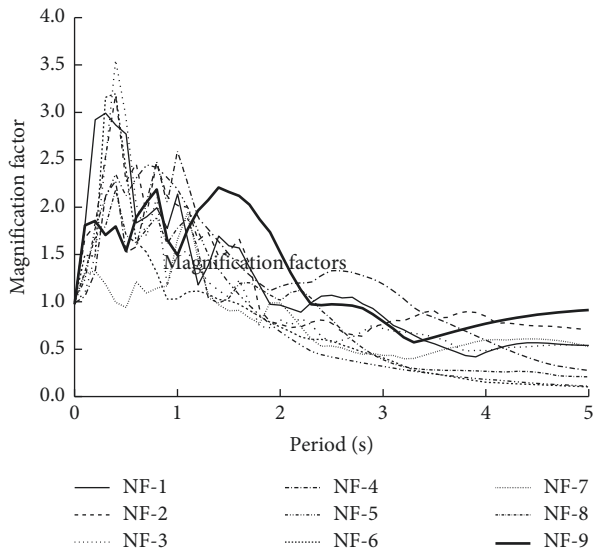

Figure 3: Response spectrum of near-fault ground motions.

4.1. Earthquake Record Inputs for Time-History Analysis. The velocity waveforms may not have pulses with the polarity reversals that make near-fault directivity pulses so destructive. According to the "Guidelines for Seismic Design of Highway Bridge" (JTG/T B02-01-2008) and "Specification of Seismic Design for Highway Engineering" (JTG B02-2013), the bridge was closed to a fault (only several kilometers) to investigate the seismic performance of the seismic isolation bridge structure under near-fault ground motions. Furthermore, nine near-fault ground-motion records with velocity pulses were specifically selected and input along the longitudinal direction of the bridge after adjusting the PGA. Table 3 lists the details of the selected near-fault earthquake waves. The near-fault ground motions were downloaded from the PEER/NGA database, and the permanent ground displacement ("fling step") effects were moved by their processing procedure of filtering, and only the rupture directivity effects were considered in the paper.

Figures 3 and 6 depict the magnified coefficient response spectrum, average spectrum of input earthquake waves, and the bridge seismic specification spectrum for category III sites. As shown in Figure 6, the average spectrum value of the selected near-fault earthquake wave was greater than the specification spectrum in the long period. Moreover, being rich in medium-period and long-period components is an important characteristic of near-fault ground motions.

4.2. Multilevel Performance Objective Assessment

4.2.1. E1 Earthquake. Note that the PGA corresponding to E1 earthquakes was 0.2 g. Figure 7 shows the displacement of girders and bearings under near-fault ground motions.

The maximum displacement of bearings under near-fault ground motions was 0.11 m, which met the requirement that the maximum shear strain of bearings should be less than 100% (see Figure 7). The maximum residual displacement of the LRBs was 37 mm, which was approximately 16% of the bearing height and primarily located in the third continuous span unit. Though the ratio of the residual displacement to bearing height exceeded the upper bound, due to the larger uncertainty in the seismic response of isolated bridge under near-fault ground motion, this value was still acceptable. However, some bearings may need replacement after earthquakes.

4.2.2. Medium Earthquake. In the combined seismic isolation system with LRBs and CDRs, it was assumed that the CDRs have enough capacities, so the seismic responses of the CDRs were not analyzed here. The seismic responses of the LRBs and the responses of the piers were concerned. Figure 8 shows the displacement response for the girder, bearing, and piers under near-fault ground motions (0.4 g). Under the effect of near-fault ground motions, the displacement of the girder and LRBs reached 0.225 m and 0.221 m, respectively. Furthermore, the shear strain of the bearing's rubber layer exceeded 1.5 (rubber thickness was 0.144 m). The displacement of piers reached yield displacement approximately.

4.2.3. E2 Earthquake. Table 4 lists the displacement response of seismically isolated bridges under the effect of 0.62 g near-fault ground motions. It was observed that the maximum shear strain of the bearings was 238%, whereas

Table 2: Mechanical characteristics of bearings.

Location	Type	K_1 (kN/m)	K_2 (kN/m)	F_y (kN)	[F] (kN)
Abutment	$GYZF_4D400\times60$	2094	0	46	1195
Expansion joint	$GYZF_4D400\times38$	3306	0	46	1195
Pier	$Y4Q770\times232$	14900	2300	216	4300

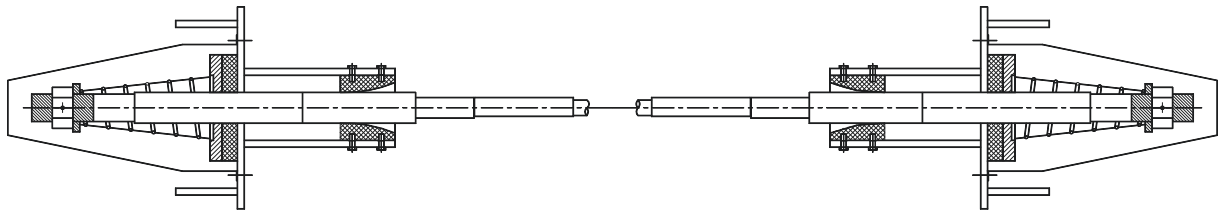

Figure 4: Cable displacement restrainers [18].

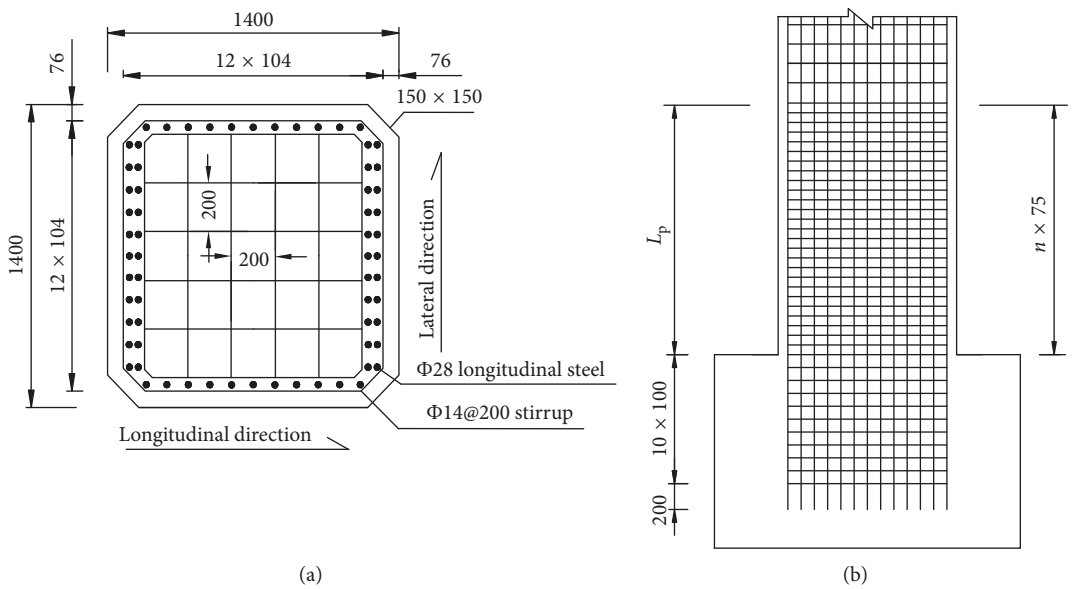

Figure 5: Arrangement of steel bars in bridge columns (unit: mm). (a) Arrangement of steel bars in the section. (b) Arrangement of steel bars in the mesh area with length L_p.

Table 3: Records of near-fault ground motions.

Number	Earthquake event	Station	PGA (g)	PGV (cm/s)	PGD (cm)
NF-1	ChiChi, 1999	TCU051-EW	0.160	51.53	124.52
NF-2	ChiChi, 1999	TCU054-EW	0.146	45.96	121.47
NF-3	ChiChi, 1999	TCU082-EW	0.226	51.54	152.35
NF-4	Northridge, 1994	JEN-022	0.424	106.22	43.06
NF-5	Northridge, 1994	RRS-228	0.838	166.05	28.78
NF-6	Northridge, 1994	SYL-360	0.843	129.71	32.68
NF-7	ChiChi, 1999	TCU065-EW	0.789	132.29	194.31
NF-8	ChiChi, 1999	TCU067-EW	0.499	97.26	186.16
NF-9	ChiChi, 1999	TCU068-NS	0.365	291.94	867.76

the maximum drift ratio of the piers was 2.05%. Thus, this design met the design performance goals that the failure of bearings would not occur and the collapse of piers would not happen. In addition the maximum internal force of a CDR was about 950 kN.

As an example, the displacement response of the no. 12 pier and its force-displacement drifts curve are depicted in Figure 9. It was found that the pier response would enter the inelastic stage, and the residual displacement would occur at the end of the earthquake.

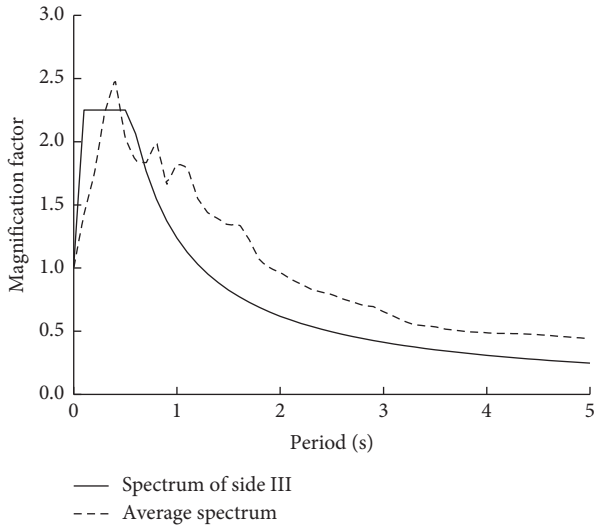

Figure 6: Average spectrum and code spectrum of site III.

5. Detailed Structural Design of Seismically Isolated Bridge

To ensure predicted performance of the seismically isolated bridge under earthquake-like conditions, the detailed structural design must be addressed. Note that the detailed structural design of this bridge is as follows.

5.1. Stirrup Ratio and Encryption Zone of Bridge Pier. Because the bridge pier was allowed to yield under E2 earthquake conditions, its stirrup design could be referenced as "08 Guidelines" and be constructed based on performance design principles. However, considering that the bridge pier should have a 3% drift ratio capacity, the value of minimum stirrup ratio should be determined based on the experimental statistical research which was studied by Sun et al. [19, 20] using 234 flexural failure RC columns. Note that Sun et al.'s study proposed a formula for the minimum stirrup ratio.

For the rectangular section piers in this paper, the adopted formulas are listed here:

$$\rho_s = \frac{A_{\mathrm{sh}}}{sh_{\mathrm{c}}} = \frac{1}{k_1} \cdot \frac{f'_{\mathrm{c}}}{f_{\mathrm{yt}}} \cdot \left(1.3 - \rho_t m\right) \cdot \eta_k \cdot \frac{A_{\mathrm{g}}}{A_{\mathrm{c}}} \geq 0.004, \quad (2)$$

$$m = \frac{f_{\mathrm{y}}}{0.85 f'_{\mathrm{c}}}, \quad (3)$$

where f_{y} is the yield strength of longitudinal reinforcement; A_{g} is the cross section area of bridge pier; A_{c} is the bridge core area calculated from the edge of the stirrup; f'_{c} is the concrete compressive strength; f_{yt} is the yield strength of the stirrup; s is the space of the stirrup; h_{c} is the depth of the cross section of the bridge pier; A_{sh} is the stirrup area of calculation cross section in s range; η_k is the axial compressive ratio; ρ_t is the longitudinal reinforcement ratio; and k_1 is the coefficient related to limiting the displacement drift under various earthquake risk levels. Note that the pier's drift ratios could reach 3%, at which $k_1 = 2.42$, and the assurance rate is 85%.

Ma et al. [21] conducted flexural-shear damage experiments for bridge pier specimens. Their results indicated that the minimum stirrup ratio calculation formula in "08 Guidelines" was still lower than that in the European and American Caltrans specifications. But the results calculated by the formula proposed by Sun et al. were similar to the stirrup ratio level in foreign seismic design specifications and were applicable to the HRB400 high-strength reinforcement. In this study, the stirrup was designed as 3% of the predicted drift ratio of the piers which are located in the high-risk earthquake region in China.

Figure 5 shows the actual stirrup of these piers (using the HRB400 high-strength stirrup). Table 5 lists the comparison of requirements on the stirrup ratios of bridge piers between the formulas proposed by Z. G. Sun, the European specification [22], the American Caltrans [23], and "08 Guidelines."

Note that the axial compression ratio η_k of the double-column piers in equation (2) might significantly change because of the transverse ground motion (overturning moment effects), and the stirrup design should use its maximum value. Researchers in this paper utilized the Midas/Civil software to perform transverse pushover analysis for the double-column piers: four typical groups of bridge piers with heights of 5, 6, 7, and 9 m were selected and loaded with the predicted drift for the bridge piers up to 3%. As part of this study, this paper has only presented the horizontal force-displacement relationship curves of the double-column piers, which was achieved by the pushover analysis for 7 m high double-column piers and the axial variation of the single bridge pier at the bottom, as shown in Figures 10 and 11.

Finally, Table 6 lists the details of the stirrup densification area under various specification requirements [24]. Considering that the contraflexure point of the bridge piers was located at the midspan and the calculated height of bridge decreased by ½, the piers beneath 7 m in this bridge were applied to the completely dense stirrups, whereas the 2.1 m range dense stirrups were applied to the situation that a potential plastic hinge was located along the pier height.

5.2. Expansion Joint Design. According to China's "Guidelines for Seismic Design of Highway Bridge," when selecting the expansion joint gap of girder, the displacement of girder should be considered under the action of earthquake. The results from the E2 earthquake during near-fault ground motions were used as a reference to optimize gaps between the longitudinal bridge connections and the bridge abutment expansion joint. Because the stiffness of the bridge abutment was much larger than that of the bridge piers which was equipped with the LRB bearings, the relative displacement response between the abutment and the adjacent girder was mainly contributed by the latter. At the expansion joint of the bridge abutment, the girder's displacement should be less than that for the expansion joint gap, whereas considering the maximum displacement

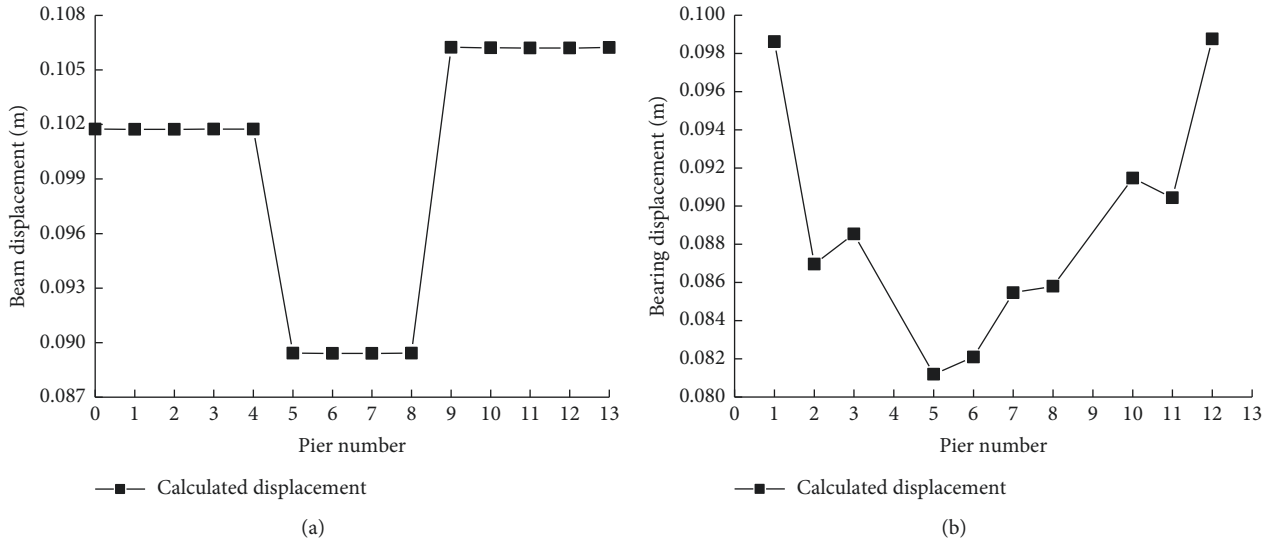

Figure 7: Displacement response of bridges under E1 earthquake. (a) Girder displacement. (b) Bearing displacement.

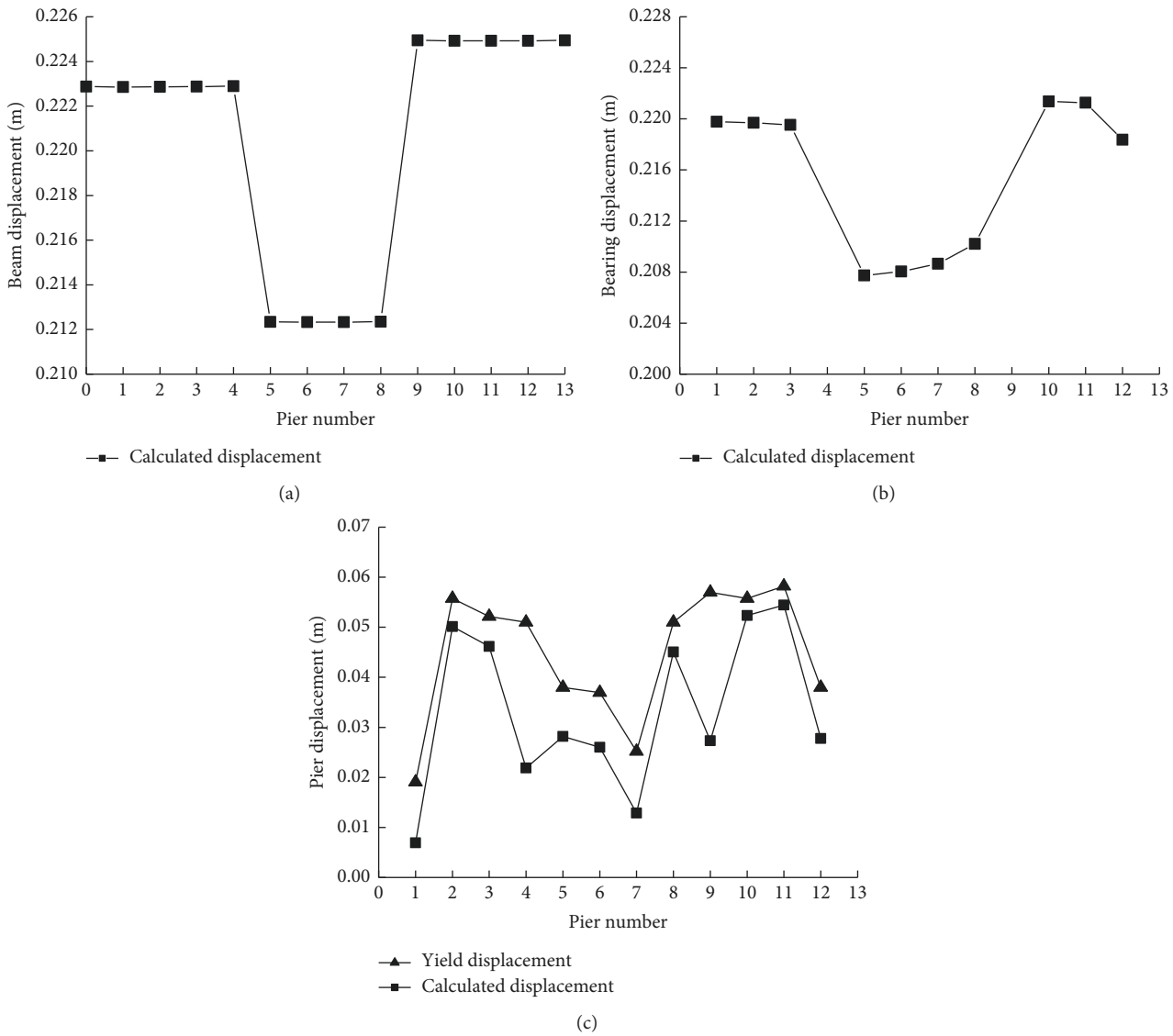

Figure 8: Displacement response under design earthquake. (a) Girder displacement. (b) Bearing displacement. (c) Pier displacement.

Table 4: Displacement response of seismically isolated bridge.

Pier location	Girder displacement (m)	Bearing displacement (m)	Pier displacement (m)	Bearing shear strain	Drift ratio of the pier (%)
1	0.381	0.342	0.110	2.38	2.05
2	0.381	0.296	0.132	2.06	1.44
3	0.381	0.296	0.131	2.05	1.48
4	0.371	—	0.035	—	0.40
5	0.371	0.287	0.110	1.99	1.46
6	0.371	0.286	0.110	1.99	1.47
7	0.371	0.341	0.021	2.37	0.35
8	0.371	0.291	0.121	2.02	1.39
9	0.371	—	0.044	—	0.47
10	0.381	0.297	0.130	2.06	1.42
11	0.381	0.296	0.130	2.06	1.39
12	0.381	0.293	0.117	2.04	1.56

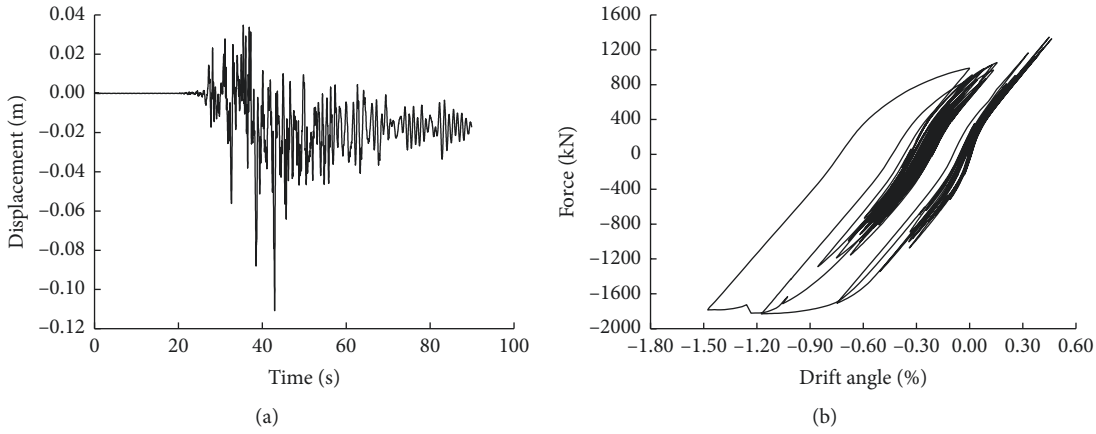

Figure 9: Response of the no. 12 pier. (a) Displacement response. (b) Force-displacement drifts curve.

(381 mm) of the girder under the action of E2 earthquake, the commercial product of the expansion joint was OVM-MF400 mm. According to China's "Guidelines for Seismic Design of Highway Bridge," the expansion joint at the middle spans could be 0.8 times that of the expansion joint at the bridge abutment, i.e., 320 mm, whereas the commercial product of expansion joint was OVM-MF320 mm. To mitigate the longitudinal pounding effects of the bridge and to prevent the girder from falling, the appropriate damping and collision-proof rubber bumpers and other measures were used in the expansion joints.

5.3. Design of Restrainer and Girders Falling-Prevention Measures. Cable restrainers were used as longitudinal displacement-limiting devices between the piers and girders. When the lead rubber bearing approached its ultimate deformation capacity, the cable displacement restrainers start to work, which protects the bearing and limits the relative displacement between pier and beam. The initial clearance of the cable displacement restrainers was 280 mm corresponding to 200% of the lead rubber bearing shear strain. The transverse displacement-limiting devices such as reinforced concrete blocks (shear keys) are also used. The minimum seating length provided by the cap girder guaranteed to prevent the falling down of the girders. Table 7 lists the semiempirical statistical results in the relative displacement spectrum model between piers and girders proposed by Wang et al. [25] The bridge was located at the category III soil site, which was close to a fault, and the support length of the cap girder between the bridge abutment and the expansion joint was 1.4 m; however, under the "08 Guidelines," this length was 0.8 m (20 m span).

5.4. Design of Vertical Displacement-Limiting Devices. The seismic isolation rubber bearings exhibited poorly tensile strength. The bridge was located in a high-intensity earthquake zone and close to a fault. Therefore, the vertical displacement-limiting device should be considered. The total design tension of the vertical displacement-limiting device was 25% of the self-weight of the superstructure; moreover, each girder was independently designed. At present, the vertical displacement-limiting devices can be designed by the steel tension cables easily; in addition, the vertical limit device adopted the cable-sliding friction aseismic bearing in China [26], and the cable in the cable-sliding friction aseismic bearing could also be used to satisfy the vertical limit under the action of the earthquake. These provisions were from those of the Caltrans in the United States [23]. The

Table 5: Comparison of the stirrup ratio.

Specification	Stirrup ratio (%) Pier height $H = 5$ m, 6 m, 7 m, 9 m
Sun's formula [16]	0.48, 0.47, 0.46, 0.44
European code EN1998-2	0.80, 0.80, 0.80, 0.80
Caltrans 2006	0.57, 0.56, 0.56, 0.56
China's guidelines	0.40, 0.40, 0.40, 0.40

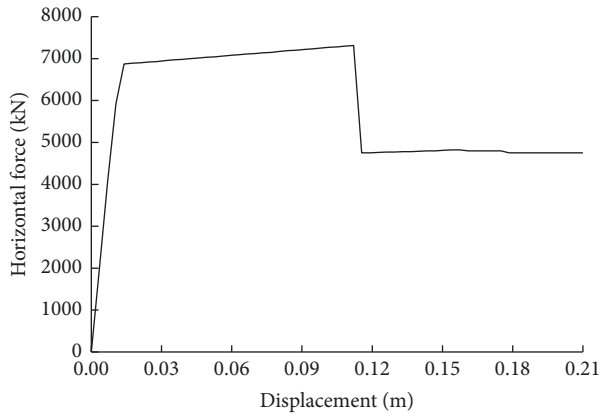

Figure 10: Horizontal force-deformation curve.

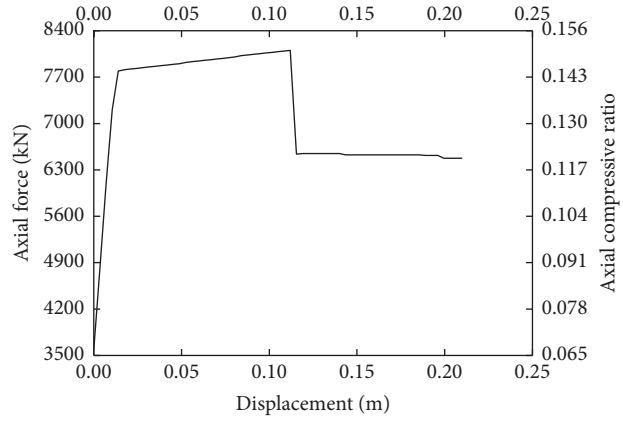

Figure 11: Axial force-deformation curve.

vertical seismic force should be considered in an area with a PGA of >0.6 g. The total design tension of the vertical displacement-limiting device should be 25% of the self-weight of the girder, whereas the direction of the tension (positive or negative) should be considered.

6. Conclusion

For designing bridges located near faults in high-intensity earthquake zones (0.4 g), this study proposed a seismic isolation design scheme that used combined seismic isolation systems of LRBs and CDRs and the ductility seismic resistance of reinforced concrete piers. Moreover, multilevel performance-based objectives were provided to design the combined seismic isolation system under the conditions of frequent earthquakes (E1), design earthquakes (medium earthquakes), and rare earthquakes (E2). This study validated the effectiveness of a performance-based seismic isolation design method using a near-fault highway bridge in the PGA 0.4 g acceleration area. Furthermore, it provided the key point of relative quantitative design in detail for the combined damping system and the ductility of the piers such as the stirrup ratios of bridge piers, expansion joint clearance, support length of capping beams, and vertical displacement-limiting devices.

Table 6: Comparison of the stirrup mesh zones.

Specification	Mesh range (m) Pier height $H = 5$ m, 6 m, 7 m, 9 m
China's guidelines	5.0, 6.0, 7.0, 1.4
Caltrans 2006	2.1, 2.1, 2.1, 2.1
European code EN1998-2	1.4, 1.4, 1.4, 1.4
Actual design	Full column, 2.1

Table 7: Minimum seating length provided by cap girder (unit: cm).

Site category	I	II	III	IV
Minimal support length	30	30	70	100
Note	"08 guidelines" design: $70 + 0.5L$ (cm), where L is the span (m)			

Note. For bridges within 10 km of an active fault, a magnifying factor of 2.0 is applied.

Data Availability

The data used to support the findings of this study are available from the corresponding author upon request.

Conflicts of Interest

The authors declare that they have no conflicts of interest.

Acknowledgments

The authors gratefully acknowledge the support for this research by the National Natural Science Foundation of China under grant nos. 51708081 and 51768042 and Natural Science Foundation of Liaoning Province under grant no. 201602066.

References

[1] P. Somerville, "Characterizing near fault ground motion for the design and evaluation of bridges," in *Proceedings of the Third National Seismic Conference and Workshop on Bridges and Highways*, MCEER Buttalo, Portland, OR, USA, May 2002.

[2] J. E. Roberts, "Caltrans structural control for bridge in high-seismic zones," *Earthquake Engineering and Structural Dynamics*, vol. 34, no. 4-5, pp. 449–470, 2005.

[3] M. O. Moroni, R. Boroschek, and M. Sarrazin, "Dynamic characteristics of chilean bridges with seismic protection," *Journal of Bridge Engineering*, vol. 10, no. 2, pp. 124–132, 2005.

[4] G. C. Lee, Y. Kitane, and I. G. Buckle, *Literature Review of the Observed Performance of Seismically Isolated Bridges*,

Multidisciplinary Center for Earthquake Engineering Research, New York, NY, USA, 2001.

[5] S. W. Park, H. Ghasemi, and J. Shen, "Simulation of the seismic performance of the Bolu viaduct subjected to near-fault ground motions," *Earthquake Engineering and Structural Dynamics*, vol. 33, no. 4, pp. 1249–1270, 2004.

[6] B. Bessason and E. Haflidason, "Recorded and numerical strong motion response of a base-isolated bridge," *Earthquake Spectra*, vol. 20, no. 2, pp. 309–332, 2004.

[7] M. H. Jónsson, B. Bessason, and E. Haflidason, "Earthquake response of a base-isolated bridge subjected to strong near-fault ground motion," *Soil Dynamics and Earthquake Engineering*, vol. 30, no. 6, pp. 447–455, 2010.

[8] M. Dicleli, "Supplemental elastic stiffness to reduce isolator displacements for seismic-isolated bridges in near-fault zones," *Engineering Structures*, vol. 29, no. 5, pp. 763–775, 2007.

[9] M. Dicleli, "Performance of seismic-isolated bridges with and without elastic-gap devices in near-fault zones," *Earthquake Engineering & Structural Dynamics*, vol. 37, no. 6, pp. 935–954, 2008.

[10] E. Osman, A. Ozbulut, and S. Hurlebaus, "Optimal design of super elastic-friction base isolators for seismic protection of highway bridges against near-field earthquakes," *Earthquake Engineering and Structural Dynamics*, vol. 40, no. 3, pp. 273–291, 2011.

[11] D. Losanno, H. A. Hadad, and G. Serino, "Seismic behavior of isolated bridges with additional damping under far-field and near fault ground motion," *Earthquakes and Structures*, vol. 13, no. 2, pp. 119–130, 2017.

[12] D. Losanno, M. Spizzuoco, and G. Serino, "Optimal design of the seismic protection system for isolated bridges," *Earthquakes and Structures*, vol. 7, no. 6, pp. 969–999, 2014.

[13] Ministry of Transport of the People's Republic of China (MTPRC), *Guidelines for Seismic Design of Highway Bridges, JTG/T B02-01-2008*, MTPRC, Beijing, China, 2008.

[14] K. Kawashima and S. Unjoh, *Menshin Design of Highway Bridges in JAPAN*, National Center for Earthquake Engineering Research, New York, NY, USA, 1994.

[15] Y. Shi, D. S. Wang, and Z. G. Sun, "Comparison and analysis of guide specifications for seismic isolation design," *Earthquake Engineering and Engineering Vibration*, vol. 35, no. 5, pp. 79–84, 2015.

[16] Y. Shi, D. S. Wang, and Z. G. Sun, "Displacement-based seismic design method for medium span bridges with seismic isolation," *China Journal of Highway and Transport*, vol. 29, no. 2, pp. 71–81, 2016.

[17] Ministry of Transport of the People's Republic of China (MTPRC), *Lead Rubber Bearing Isolator for Highway Bridge, JT/T822-2011*, MTPRC, Beijing, China, 2012.

[18] W. X. Zhu, J. P. Ou, Y. Huang et al., "A new type cable restrainer for prevention of unseating damage of bridge superstructures," *Journal of Pre-stress Technology*, vol. 6, no. 5, pp. 3–7, 2008.

[19] Z. G. Sun, D. S. Wang, and X. Guo, "Research on equivalent plastic hinge length of reinforced concrete bridge column," *China Journal of Highway and Transport*, vol. 24, no. 5, pp. 56–64, 2011.

[20] Z. G. Sun, D. S. Wang, and X. L. Du, "Research on amount of confining reinforcement in potential plastic hinge regions of RC bridge columns," *China Journal of Highway and Transport*, vol. 23, no. 3, pp. 48–57, 2010.

[21] Y. Ma, Z. G. Sun, and D. S. Wang, "Evaluation of amounts of confining stirrups used for RC bridge columns based on deformation capacity," *Bridge Construction*, vol. 44, no. 6, pp. 57–62, 2014.

[22] European Committee for Standardization (CEN), *Eurocode 8, Design Provisions for Earthquake Resistance of Structures-Part 2: Bridges*, CEN, Brussels, Belgium, 1998.

[23] California DOT (Caltrans), *Seismic Design Criteria, Version 1.4*, Caltrans, Sacramento, CA, USA, 2006.

[24] J. X. Gong, Q. Zhang, and X. T. Wang, "Comparative study on bridge seismic design approaches in different specifications based on survey of disaster in Wenchuan earthquake(2)," *Journal of Highway and Transportation Research and Development*, vol. 27, no. 10, pp. 35–46, 2010.

[25] D. S. Wang, Z. G. Sun, and X. Guo, "Lessons learned from Wenchuan seismic damages and recent research on seismic design of highway bridges," *Journal of Highway and Transportation Research and Development*, vol. 28, no. 10, pp. 44–53, 2011.

[26] W. C. Yuan, Z. H. Wei, X. J. Cao, and Z. J. Rong, "Cable-sliding friction aseismic bearing and its application in bridge seismic design," *Engineering Mechanics*, vol. 28, no. 2, pp. 204–209, 2011.